

Kondo effect of impurity moments in d -wave superconductors: Quantum phase transition and spectral properties

Matthias Vojta and Ralf Bulla

*Theoretische Physik III, Elektronische Korrelationen und Magnetismus, Institut für Physik, Universität Augsburg,
D-86135 Augsburg, Germany*

(Received 15 August 2001; published 4 December 2001)

We discuss the dynamics of magnetic moments in d -wave superconductors. In particular, we focus on moments induced by doping nonmagnetic impurities into cuprates. The interaction of such moments with the Bogoliubov quasiparticles of the superconductors can be described by variants of the pseudogap Kondo model, characterized by a power-law density of states at the Fermi level. The numerical renormalization-group technique is employed to investigate this Kondo problem for realistic band structures and particle-hole asymmetries, both at zero and finite temperatures. In particular, we study the boundary quantum phase transition between the local-moment and asymmetric strong-coupling phases, and argue that this transition has been observed in recent nuclear magnetic resonance experiments. We determine the spectral properties of both phases and the location of the critical point as a function of Kondo coupling and doping, and discuss quantum-critical crossovers near this phase transition. In addition, changes in the local density of states around the impurity are calculated as functions of temperature, being relevant to scanning tunneling microscopy experiments.

DOI: 10.1103/PhysRevB.65.014511

PACS number(s): 74.72.-h, 74.25.Jb, 75.20.Hr, 71.27.+a

I. INTRODUCTION

Impurities have proven to be a powerful probe for investigating the bulk behavior of complex many-body systems. In the field of high-temperature superconductivity, a variety of phenomena has been observed under doping with magnetic as well as nonmagnetic impurities: a suppression of the superconducting critical temperature T_c and an increase of the residual in-plane resistivity,^{1,2} a damping of collective magnetic excitations (the so-called resonance mode³), a possible pinning of stripes and vortices, and impurity-related local bound states seen in scanning tunneling microscopy (STM).⁴⁻⁶

A particularly interesting piece of physics is the magnetism of impurities which are substituted for Cu ions. Experiments have been performed with magnetic spin-1 (Ni) as well as nonmagnetic spin-0 (Zn, Li) impurities. Whereas the spin-1 impurities naturally carry an on-site moment which is expected to give rise to some kind of Kondo physics, the behavior of nonmagnetic impurities is more surprising. A series of nuclear magnetic resonance (NMR) experiments⁷⁻¹⁴ clearly showed that each impurity, despite having no on-site spin, induces a local $S=1/2$ moment on the neighboring Cu ions at intermediate energy scales. In particular, the local susceptibility associated with Li ions in $\text{YBa}_2\text{Cu}_3\text{O}_{6+x}$ (YBCO) has been found to show a Curie-Weiss-like behavior, with a strongly doping dependent Weiss temperature which appears to vanish for strongly underdoped samples—this implies the existence of free moments in the underdoped regime down to temperatures of order 1 K. Microscopic perspectives on the formation of these local impurity moments will be discussed in Sec. II.

Accepting that nonmagnetic impurities induce local moments, these moments are expected to interact with the elementary excitations of the bulk material.¹⁵ In this paper, we will be mainly concerned with a d -wave superconducting bulk state, i.e., with temperatures T below the superconduct-

ing T_c : the relevant low-energy excitations of the d -wave superconductor are fermionic Bogoliubov quasiparticles and bosonic antiferromagnetic spin fluctuations (as seen in neutron scattering); quantum phase fluctuations which may become important near a superconductor-insulator quantum phase transition will not be considered here. The interactions of impurity moments with fermionic and bosonic degrees of freedom can be discussed separately, as they lead to distinct phenomena associated with fermionic and bosonic Kondo models. Also, the energy scales of these two phenomena appear to be well separated, as the fermionic Kondo temperature in the superconducting state is below 100 K whereas the spin fluctuation energy scale is given by the energy of the “resonance mode,”³ which is 40 meV at optimal doping.

The interaction of an impurity spin with bosonic spin-1 fluctuations of a quantum disordered antiferromagnet is described by a “bosonic Kondo model.”¹⁶⁻¹⁸ It was recently studied in the context of impurities in two-dimensional nearly critical antiferromagnets, where it leads to a (2+1)-dimensional boundary quantum field theory with a number of interesting universal properties.¹⁶ If the bulk state has a finite spin gap, then the impurity moment is not screened, i.e., it contributes with a Curie term to the impurity susceptibility. However, the moment is spatially “smeared” over a length scale given by the magnetic correlation length, i.e., part of the moment is carried by neighboring spins. Another result of Ref. 16 was that a finite concentration of impurity moments leads to a universal damping of the collective spin-1 mode of the bulk magnet. Together with recent neutron-scattering experiments,³ this provides further evidence of $S=1/2$ induced local moments near Zn sites in cuprate superconductors: it was argued¹⁶ that these moments are required to explain the strong effects of a small concentration of Zn impurities on the “resonance peak” in the spin dynamic structure factor.

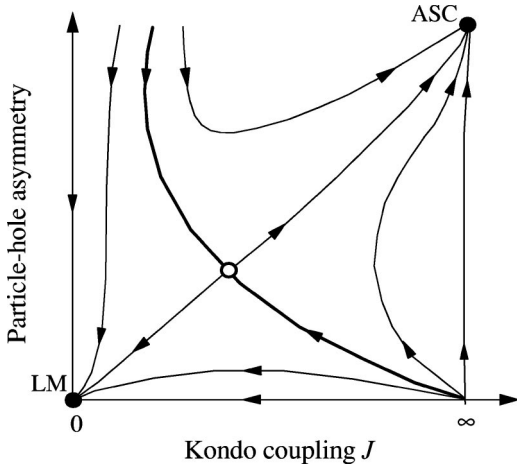


FIG. 1. Schematic zero-temperature renormalization-group flow diagram (Ref. 26) for the pseudogap Kondo model with a power-law density of states $\rho(\epsilon) \sim |\epsilon|^r$ with $r > 1/2$. The horizontal axis denotes the Kondo coupling, the vertical axis denotes particle-hole asymmetry (parametrized, e.g., by the potential scattering strength U for a particle-hole symmetric host band structure). The model has two stable fixed points (solid dots): the weak-coupling local moment (LM) fixed point, where the impurity is essentially decoupled from the band, and the asymmetric strong coupling (ASC) fixed point, where the impurity moment is fully screened. The thick line represents the second-order phase transition between the two zero-temperature phases, and the open dot is the critical fixed point. Note that there is no screening in the particle-hole symmetric case even for infinitely strong Kondo coupling.

In this paper, we will focus on the interaction of the impurity moment with the *fermionic* bulk degrees of freedom, namely, the quasiparticles of the *d*-wave superconductor. Importantly, the single-particle density of states (DOS) of the Bogoliubov quasiparticles vanishes at the Fermi energy, and so we expect a number of features quite distinct from the usual Kondo effect in metals.¹⁹ The Kondo effect in systems where the host DOS follows a power law near the Fermi level, $\rho(\epsilon) \sim |\epsilon|^r$ ($r > 0$), was studied quite extensively in the context of the pseudogap Kondo model.^{20–30} A number of studies,^{20,21,28,29} including the initial work of Withoff and Fradkin, employed a slave-boson large- N technique;³¹ further progress and insight came from numerical-renormalization-group (NRG) calculations,^{23–26} the local-moment approach,²⁷ and a dynamic large- N method.³⁰ The general picture arising from these studies is that there exists a zero-temperature (boundary) phase transition at a critical Kondo coupling J_c , below which the impurity spin is unscreened even at lowest temperatures. Also, the behavior depends sensitively on the presence or absence of particle-hole symmetry: in the particle-hole symmetric case there is no complete screening even for Kondo couplings $J > J_c$. A comprehensive discussion of possible fixed points and their thermodynamic properties was given by Gonzalez-Buxton and Ingersent²⁶ based on the NRG approach. Figure 1 summarizes their findings for $r > 1/2$, including the case $r = 1$ relevant for *d*-wave superconductors (also see Fig. 16 of Ref. 26).

Spectral properties of the pseudogap Kondo model [for

the relevant case of SU(2) spin symmetry] have so far been investigated for the particle-hole symmetric case only.^{24,27} However, interesting properties are to be expected especially for the asymmetric case, considering the results of static^{20,21,28} and dynamic³⁰ large- N approaches.

The study of spectral properties of Kondo impurities in metals as well as in superconductors has been revived due to recent advances in STM. Tunneling to clean surfaces of materials with bulk or surface impurities has made it possible to directly observe local spectral properties associated with impurities. In particular, Kondo impurities on metal surfaces have been found to give rise to a *dip* or Fano-like line shape in the tunneling DOS.^{32,33} In contrast, in cuprate *d*-wave superconductors *peak* structures in the local DOS close to the Fermi energy have been found for both Zn and Ni impurities^{4–6} doped into $\text{Bi}_2\text{Sr}_2\text{CaCu}_2\text{O}_{8+\delta}$ (BSCCO). Whereas the results for Ni appear to be well described by a model with combined potential and static magnetic (spin-dependent) scattering,³⁴ the signal of Zn impurities—a huge tunneling peak at energies of 1–2 meV—is more puzzling. It is tempting to identify this peak with a quasibound state in a purely potential scattering model,^{34–38} but such a state appears at low energies only for a range of very large potential values depending upon microscopic details.^{34,39,40} Furthermore, the spatial dependence of the zero bias peak is surprising—see further discussion in Sec. V—and the observed spatially integrated spectrum is asymmetric between positive and negative bias,⁴ while the potential model predicts approximate symmetry.⁴¹ Recently, it was proposed⁴² that some of the properties of the Zn resonance can be explained by taking into account the Kondo spin dynamics of the magnetic moment induced by Zn. The screening of this moment by the Boboliubov quasiparticles provides a natural low-energy scale (the Kondo temperature) explaining the energetic location of the peak seen in STM.

The purpose of this paper is twofold: On the one hand we want to study the fermionic pseudogap Kondo effect using realistic band structures for the cuprates. We shall show that the transition between a free moment and a screened moment in the pseudogap Kondo model can be driven by varying doping in the high- T_c compounds—this provides an explanation for the strong doping dependence of the Kondo (Weiss) temperature observed in NMR.^{12,13} On the other hand, we want to examine a number of properties of the pseudogap Kondo model close to this transition, and relate them to experimental findings, in particular STM measurements.

The remaining part of the paper is organized as follows. In Sec. II we briefly discuss the issue of properly modeling a nonmagnetic impurity in cuprates—we will motivate the model consisting of a Kondo and a potential scattering term, and further discuss a number of theoretical aspects in Sec. III. In Sec. IV we turn to the simplest model, namely, a pointlike magnetic impurity with a realistic host density of states (taking dispersion and gap data of actual cuprate materials). Using the numerical renormalization-group method, we will discuss static and dynamic properties of the two stable fixed points as well as of the quantum critical regime. We will determine the critical coupling constant and the

crossover scale as function of doping, and make contact with the transition seen in NMR experiments. In Sec. V we extend the impurity modeling to a spatially distributed magnetic moment and additional potential scattering and present in particular the resulting local conduction electron DOS which is relevant for STM experiments. A brief discussion of open issues will close the paper.

Parts of the discussion in Sec. II were already given in Refs. 42 and 43, but we decided to include them here to keep the paper self-contained. Readers mainly interested in the experimental consequences for cuprates might skip the technical issues in Sec. III, and have a look at Sec. IV C (especially Fig. 9), as well as Secs. IV B 2 and V which are related to STM observations.

II. EFFECTIVE MODELS FOR NONMAGNETIC IMPURITIES

As NMR experiments show, nonmagnetic impurities can induce local moments in correlated hosts. In this section we will briefly discuss theoretical perspectives on this phenomenon.

To describe a nonmagnetic impurity in a strongly correlated superconducting system, two approaches appear possible. (i) One starts with a basic model for the bulk system containing correlation terms, e.g., a one- or three-band Hubbard model with strong on-site interaction, and describes the nonmagnetic impurity by a potential scattering term as suggested by its chemistry. This approach is notoriously difficult, as a strongly correlated model (which is hard to deal with even without impurity) has to be treated including the impurity and in the low-temperature limit. This task is almost impossible for current numerical techniques such as Monte Carlo or exact diagonalization,⁴⁴ and analytical approaches suffer from uncontrolled approximations. (ii) One separates the questions of moment formation and interaction of the moment with the bulk system. To describe the latter, one can employ *effective* models for both the impurity and the bulk system. The model for the bulk system has to contain only the minimal ingredients to describe the desired low-temperature physics—in the present case this is a d -wave BCS model which does not contain correlation effects other than the Hartree-Fock pairing term. The impurity term of the effective model has to account for the correlation effects related to the introduction of the impurity—in the case of interest it has (at least) to contain the magnetic moment and a scattering potential.

In this discussion and the rest of the paper, we will adopt approach (ii); also see Ref. 43. Therefore, we will not attempt a rigorous derivation showing the existence of the magnetic moment near the nonmagnetic impurity, but instead give some plausible arguments for its appearance. If we consider an undoped paramagnetic Mott insulator as reference system at $T=0$, the moment formation is easily seen to arise from breaking singlets^{7,45} by removing spins. These unpaired spins will remain in the vicinity of the impurities if the host antiferromagnet has *confined* spinons, i.e., elementary spin-1 excitations. In this picture each impurity can be understood as a localized “holon” which binds the moment of a S

$=1/2$ “spinon.” By continuity, the described mechanism is also expected to be effective at small, but finite hole doping. At larger doping, a related picture can be developed by analogy with the theory⁴⁶ for moment formation in the disordered metallic state of Si:P—small variations in the potential combine with strong local correlations to induce very localized spin excitations. Other theoretical perspectives^{47–50} on local-moment formation in the cuprates have also been given—most of them are based on the related idea that strong potential scatterers can form quasi-bound states at the impurity sites near the Fermi level.⁴⁸ Accounting for the strong local Coulomb repulsion, each bound state will capture only a single electron, and the low-energy physics will again be described by an impurity spin model.

It is evident that the magnetic properties associated with the induced moment will depend strongly on the hole doping level. The undoped limit, i.e., the undoped paramagnetic Mott insulator, has a free $S=1/2$ moment near each impurity, while the strongly doped limit (where electronic correlations are presumably weak) does not. From continuity one expects that the free $T=0$ moment will survive in the superconducting state for a finite range of doping; spin quantization suggests that the size of the moment as measured by the Curie term in the susceptibility is always $S=1/2$ independent of doping, i.e., each moment will contribute a divergent Curie susceptibility $\sim 1/4T$ even in the (underdoped) superconducting state. Then, a quantum critical point separates the weak and strong doping limits. On the strong doping side of this quantum critical point, the moment is Kondo screened as $T \rightarrow 0$, and such a regime is continuously connected to a regime, at higher doping, where the moment does not even form at intermediate T . We wish to argue that this quantum phase transition is precisely the transition present in the pseudogap Kondo model, and this claim is supported by quantitative calculations in Sec. IV.

We note that the pictures of the moment formation quoted above do not give reliable information about the parameters of a possible effective impurity model. NMR suggests that the magnetic moment is spatially distributed among the Cu sites near the impurity (but fluctuates as a single entity). However, the precise microscopic form of the coupling between the spin moment and the conduction electrons is not known — one has to keep in mind that the moment is formed by a particular (bound) state of the conduction electrons near the impurity, and it interacts with the other states (i.e., linear combinations) of the *same* conduction electrons. In the absence of a precise knowledge of the appropriate microscopic model, we will employ some simple Anderson- and Kondo-like models for the impurities which are discussed in the following section.

III. MICROSCOPIC MODELS AND METHODS

For the remainder of this paper we restrict our attention to effective low-energy models consisting of a BCS-like d -wave superconductor, a scattering potential, and a magnetic moment, $\mathcal{H} = \mathcal{H}_{\text{BCS}} + \mathcal{H}_{\text{pot}} + \mathcal{H}_{\text{mag}}$. In particular, we neglect the strong short-range magnetic correlations of the bulk material. As mentioned in Sec. I, these low-energy magnetic

fluctuations couple to the impurity moment leading to a bosonic Kondo model. Due to the nonzero spin gap, the main effect of this coupling is an additional spatial “smearing” of each impurity moment, which can be absorbed in the effective impurity model.

We assume that the cuprate superconductor can be described within BCS theory, so we use

$$\mathcal{H}_{\text{BCS}} = \sum_{\mathbf{k}} \Psi_{\mathbf{k}}^{\dagger} [(\varepsilon_{\mathbf{k}} - \mu)\tau^z + \Delta_{\mathbf{k}}\tau^x] \Psi_{\mathbf{k}}. \quad (1)$$

Here $\Psi_{\mathbf{k}} = (c_{\mathbf{k}\uparrow}, c_{-\mathbf{k}\downarrow}^{\dagger})$ is a Nambu spinor at momentum $\mathbf{k} = (k_x, k_y)$ ($c_{\mathbf{k}\alpha}$ annihilates an electron with spin α on a Cu $3d$ orbital), $\tau^{x,y,z}$ are Pauli matrices in particle-hole space, and μ is the chemical potential. For the kinetic energy $\varepsilon_{\mathbf{k}}$, we will use a tight-binding form which includes nearest-neighbor hopping as well as longer-range hopping processes,⁵¹ while we assume a d -wave form for the BCS pairing function, $\Delta_{\mathbf{k}} = (\Delta_0/2)(\cos k_x - \cos k_y)$.

In the numerical calculations of this paper we will neglect order-parameter relaxation due to the impurity. This effect might play a role for strong scattering potentials, in that it suppresses the magnitude of the gap and leads to a finite zero-energy DOS. However, STM experiments^{4,5} showed that the local change in the gap size is rather small. Furthermore, the induced zero-energy DOS will also be small, and the resulting (finite) Kondo temperature will be exponentially suppressed. So we expect results including order-parameter relaxation to be similar to ours below, at least regarding the magnetic properties of the impurity in the experimentally accessible temperature range.

A. Anderson vs Kondo model

An effective model for a (magnetic or nonmagnetic) impurity consists of a potential scattering term and a magnetic term. The potential scattering term is assumed to be localized at the impurity site:

$$\mathcal{H}_{\text{pot}} = U \sum_{\sigma} c_{0\sigma}^{\dagger} c_{0\sigma}. \quad (2)$$

The problem of a single scatterer can be solved exactly, with the standard result for the Ψ Green’s function in Nambu notation:

$$\begin{aligned} G(\mathbf{r}, \mathbf{r}', \omega) &= G^0(\mathbf{r} - \mathbf{r}', \omega) - U G^0(\mathbf{r} - \mathbf{r}_0, \omega) \\ &\quad \times \tau^z [1 + U G^0((0,0), \omega) \tau^z]^{-1} G^0(\mathbf{r}_0 - \mathbf{r}', \omega); \end{aligned} \quad (3)$$

G^0 is the Green’s function of the host, $N_s G^0(\mathbf{r}, \omega) = \sum_{\mathbf{k}} e^{i\mathbf{k}\cdot\mathbf{r}} [\omega - (\varepsilon_{\mathbf{k}} - \mu)\tau^z - \Delta_{\mathbf{k}}\tau^x]^{-1}$, and $\mathbf{r}_0 = (0,0)$ is the scattering site.

The magnetic moment can be either coupled to a single site (point-like impurity) or be spatially distributed. For a pointlike magnetic impurity coupled to a single site $\mathbf{r} = (0,0)$ of a (metallic or superconducting) host, the most general form is a single-impurity Anderson model:

$$\mathcal{H}_{\text{mag}} = \sum_{\sigma} V_0 (f_{\sigma}^{\dagger} c_{0\sigma} + \text{H.c.}) + \epsilon_f \sum_{\sigma} f_{\sigma}^{\dagger} f_{\sigma} + U_f n_{f\uparrow} n_{f\downarrow}. \quad (4)$$

In the so-called Kondo limit, $V_0 \rightarrow \infty$, $\epsilon_f \rightarrow -\infty$, and $U \rightarrow \infty$, charge fluctuations on the impurity orbital are frozen, and the Anderson model can be mapped onto a Kondo model (Schrieffer-Wolff transformation),

$$\mathcal{H}_{\text{mag}} = J \mathbf{S} \cdot \mathbf{s}_0, \quad (5)$$

where $\mathbf{s}_0 = N^{-1} \sum_{\mathbf{k}\mathbf{k}'\alpha\beta} c_{\mathbf{k}\alpha}^{\dagger} \frac{1}{2} \boldsymbol{\sigma}_{\alpha\beta} c_{\mathbf{k}'\beta}$ is the conduction band spin operator at the impurity site $\mathbf{r}_0 = (0,0)$, N the number of lattice sites, and $J = 2V_0^2(1/|\epsilon_f| + 1/|U_f + \epsilon_f|)$. For $U_f/2 \neq -\epsilon_f$ this mapping also introduces an additional potential scattering term which can be absorbed in U (2).

Both models allow for a straightforward generalization to spatially distributed impurities, which are, however, no longer equivalent. The Anderson model

$$\mathcal{H}_{\text{mag}} = \sum_{\mathbf{R}\sigma} V_{\mathbf{R}} (f_{\sigma}^{\dagger} c_{\mathbf{R}\sigma} + \text{H.c.}) + \epsilon_f \sum_{\sigma} f_{\sigma}^{\dagger} f_{\sigma} + U_f n_{f\uparrow} n_{f\downarrow} \quad (6)$$

is easily seen to describe an Anderson impurity coupled to a single linear combination of conduction electrons on the sites \mathbf{R} , $\tilde{c} = \sum_{\mathbf{R}} V_{\mathbf{R}} c_{\mathbf{R}} / V$ where $V^2 = \sum_{\mathbf{R}} V_{\mathbf{R}}^2$. In the Kondo limit, such a model maps onto a Kondo model with nonlocal Kondo couplings. In contrast, the straightforward generalization of the Kondo model [Eq. (5)] to an extended impurity reads

$$\mathcal{H}_{\text{mag}} = \sum_{\mathbf{R}} J_{\mathbf{R}} \mathbf{S} \cdot \mathbf{s}_{\mathbf{R}}; \quad (7)$$

this model represents a multichannel Kondo model.^{52,53} The impurity spin couples to all possible linear combinations of the conduction electrons on the \mathbf{R} sites. In other words, a spatially extended Kondo impurity generically couples to different angular momentum channels of the conduction electrons.

The relation between models (6) and (7) was recently discussed in Ref. 54. It was argued that in an Anderson model like Eq. (6) the coupling to a *correlated* host opens new screening channels, and the effective model will be a multichannel Kondo model [Eq. (7)]. The main idea is that conduction-band correlations reduce charge fluctuations in the host, and, if an electron hops onto the impurity site, it has to hop back preferentially onto the same conduction-band site from which it came.

We note that the different screening channels generated by such a mechanism are certainly not equivalent, and the low- T behavior will be determined by a single-channel fixed point. (However, this does not exclude that genuine multichannel physics may be realized at intermediate temperatures.) We will employ a Kondo model of the form of Eq. (7) in Sec. V when discussing STM experiments on Zn in BSCCO.

B. Influence of superconducting correlations

A Hamiltonian of the form $\mathcal{H}_{\text{BCS}} + \mathcal{H}_{\text{mag}}$ not only describes a host with a pseudogap density of states, but also contains superconducting correlations. From diagrammatic perturbation theory it is clear that the Kondo problem in a normal-state system with a power-law DOS (e.g., a semimetal) is not equivalent to the Kondo problem in a superconductor with the same DOS—in other words, anomalous Green's function contribute to the screening.

For the special case of a pointlike Kondo impurity in an s -wave superconductor, however, it was shown⁵⁵ that the problem with anomalous Green's functions can be mapped onto a Kondo problem in a normal-state system with a modified gapped DOS, containing an additional particle-hole asymmetry (i.e., a potential scattering term), but without anomalous Green's functions.

In d -wave superconductors such a mapping has not been achieved so far, and the situation is less clear because the anomalous Green's functions of the d -wave superconductor provide a coupling between different angular momentum channels. Therefore, it is expected that the Kondo problem in a d -wave superconductor involves infinitely many bands (angular momenta) even for a pointlike impurity.

Various approximate methods which have been employed for solving the Kondo problem in a d -wave superconductor handle the anomalous Green's functions differently. Most calculations turn out to be insensitive to superconducting correlations in the host material, i.e., they treat a semimetal rather than a superconductor.

For instance, in the standard slave-boson approach, anomalous terms are formally included; however, for a pointlike impurity in a d -wave superconductor their contributions are easily seen to drop out. The standard implementation of the numerical renormalization-group method uses the host density of states as the only input, and anomalous terms are ignored. Based on the results for s -wave superconductors, we nevertheless expect that the results obtained by the NRG method are at least qualitatively correct in a generic particle-hole asymmetric situation, as the main influence of the anomalous Green's functions is possibly an additional particle-hole asymmetry.

C. Numerical renormalization-group method

The NRG method was developed by Wilson for an investigation of the Kondo model.⁵⁶ Due to the logarithmic discretization of the conduction band, it is able to access arbitrarily low energy scales, which is also essential for the model discussed in this paper. (However, due to the logarithmic discretization it is not possible to resolve sharp structures at high energies.) The NRG method is a nonperturbative method, as the impurity site including the strong local Coulomb interaction is treated exactly.

The NRG method was generalized to a number of different impurity models, such as the pseudogap Kondo and Anderson models.^{23–26} For these models, the main modification is the mapping of a nonconstant conduction electron density of states onto a semi-infinite chain form (see, e.g., Ref. 24).

Recently the NRG method was extended to the calculation of dynamic properties at finite temperatures; we refer the reader to Ref. 57 for details. We should mention here that information on spectral quantities for frequencies $\omega \ll T$ cannot be determined from the NRG method; the resolution is limited by the temperature and possible structures at frequencies much smaller than the temperature are missed by this approach. However, this causes no problem when comparing with, e.g., STM experiments, because the finite temperature in both the sample and tip introduces a thermal broadening, such that structures on scales smaller than T will not be resolved. The NRG calculations presented in this paper are mostly performed with a discretization parameter $\Lambda = 2$ and 600 or 800 levels.

D. Slave-boson mean-field approximation

The slave-boson mean-field approximation³¹ to the Kondo impurity model is a large- N approach, i.e., it becomes exact in the limit of large spin degeneracy $N \rightarrow \infty$. It is known that this method is not quantitatively accurate for the physical case $N = 2$, and has numerous artifacts, both at finite temperatures in general as well as near the quantum-critical point in the pseudogap Kondo model. However, it is expected to capture the qualitative physics in a Kondo screened phase. The method was applied in a number of papers to the pseudogap Kondo model,^{20,21,28,29} and we will mention some results below.

IV. POINTLIKE MAGNETIC IMPURITIES

In this section, we discuss general properties of the asymmetric pseudogap Kondo model, in particular the quantum phase transition between the local-moment and the asymmetric strong-coupling phases. Since we are mainly interested in the universal properties near this transition, we restrict our attention here to a $S = \frac{1}{2}$ impurity coupled to a pseudogap band structure, and give most results for general values of the pseudogap exponent $1/2 < r \leq 1$ (some results are also valid for $0 < r \leq 1/2$). We will obtain numerical results using the NRG method, where the DOS is the only host quantity entering the calculation. For technical purposes, namely, a convenient calculation of the impurity spectral function (or T matrix), the impurity is modeled by an Anderson Hamiltonian [Eq. (4)] (instead of a Kondo Hamiltonian) with $U_f = -2\epsilon_f$, and parameters $|U_f|, |\epsilon_f|$ much greater than the bandwidth, which places the model in the Kondo limit.⁵⁸

When specifying the results for high- T_c compounds, we consider an impurity coupled locally to a single site of the host d -wave superconductor. To obtain quantitative estimates for characteristic energies, we use tight-binding hopping parameters extracted from normal-state angle-resolved photoemission (ARPES) data⁵¹ and sizes of the d -wave gap as obtained from a number of tunneling and ARPES experiments in the superconducting state.^{59,60}

A. Zero-temperature phase transition and static properties

As discussed in a number of papers over the last years,^{20–30} the pseudogap Kondo model [with a power-law

DOS $\rho(\epsilon) \sim |\epsilon|^r$ shows a phase transition as a function of the Kondo coupling. For pseudogap exponents $r > 1/2$ there are two stable zero-temperature fixed points,²⁶ namely, (i) a local-moment (LM) regime is reached for weak initial coupling—here J flows to zero, and the impurity is unscreened—and (ii) an asymmetric strong-coupling (ASC) regime which is reached only for sufficiently large Kondo coupling and particle-hole symmetry breaking. The renormalization group flow is sketched in Fig. 1.

Particle-hole asymmetry is a relevant parameter in the pseudogap Kondo problem, as seen in Fig. 1. For a particle-hole symmetric host band structure, it can be parametrized by the amount of potential scattering at the impurity. In the general case of an asymmetric host, particle-hole asymmetry can still be cast into a *single* number, in the case of a point like Kondo impurity the real part of the local host Green's function (after inclusion of potential scattering) is a suitable choice. We will see below that, e.g., the location of the ‘‘Kondo’’ peak will depend on the sign of this overall particle-hole asymmetry. Concerning the cuprates, this overall sign cannot be extracted from experiments or theory, as it depends on details of the two-dimensional band structure which place the van Hove singularity either below or above the Fermi level. (Remarkably, this van Hove singularity has never been observed experimentally.)

For the following discussion, it is useful to define susceptibilities describing the response to external magnetic fields. We allow for a space-dependent field H_u coupled to the host and a local field H_{imp} at the impurity,

$$\begin{aligned} \mathcal{H}_{\text{BCS}} &\rightarrow \mathcal{H}_{\text{BCS}} - \sum_{i\beta\gamma} H_{u,\alpha}(i) c_{i\beta}^\dagger \sigma_{\beta\gamma}^\alpha c_{i\gamma}, \\ \mathcal{H}_{\text{mag}} &\rightarrow \mathcal{H}_{\text{mag}} - H_{\text{imp},\alpha} S_\alpha. \end{aligned} \quad (8)$$

With these definitions, a space-independent uniform field applied to the whole system corresponds to $H_u(i) = H_{\text{imp}} = H$. Response functions can be defined from derivatives of the free energy, $F = -T \ln Z$ ($k_B = 1$), as follows:

$$\begin{aligned} \chi_{u,u}(i,i') &= \frac{T}{3} \frac{\delta^2 \ln Z}{\delta H_{u\alpha}(i) \delta H_{u\alpha}(i')}, \\ \chi_{u,\text{imp}}(i) &= \frac{T}{3} \frac{\delta^2 \ln Z}{\delta H_{u\alpha}(i) \delta H_{\text{imp},\alpha}}, \\ \chi_{\text{imp,imp}} &= \frac{T}{3} \frac{\delta^2 \ln Z}{\delta H_{\text{imp},\alpha} \delta H_{\text{imp},\alpha}}. \end{aligned} \quad (9)$$

From these quantities we can define various observables, starting with the impurity contribution to the total susceptibility,

$$\begin{aligned} \chi_{\text{imp}}(T) &= \chi_{\text{imp,imp}} + 2 \sum_i \chi_{u,\text{imp}}(i) \\ &\quad + \sum_{i,i'} [\chi_{u,u}(i,i') - \chi_{u,u}^{\text{bulk}}(i,i')], \end{aligned} \quad (10)$$

where $\chi_{u,u}^{\text{bulk}}$ is the susceptibility of the bulk system in the absence of impurities. The local impurity susceptibility, i.e., the response of the impurity spin to a local field, is given by

$$\chi_{\text{loc}}(T) = \chi_{\text{imp,imp}}, \quad (11)$$

which is equivalent to the zero-frequency impurity spin autocorrelation function. Importantly, NMR Knight shift experiments measure a different quantity—there a uniform field is applied to the whole sample, and the local response is given by

$$\chi_{\text{NMR}}(T) = \chi_{\text{imp,imp}} + \sum_i \chi_{u,\text{imp}}(i). \quad (12)$$

Note that sometimes this quantity is referred to as ‘‘local susceptibility,’’ e.g., in Ref. 22.

After having defined the susceptibilities, we return to the pseudogap Kondo problem. We briefly recall the impurity thermodynamic properties of the relevant stable fixed points (LM and ASC)—these were given, e.g., in Ref. 26. The local-moment fixed point has all characteristics of a decoupled spin-1/2: susceptibility $T\chi_{\text{imp}} = 1/4$, entropy $S_{\text{imp}} = \ln 2$, and specific heat $C_{\text{imp}} = 0$. At the asymmetric strong-coupling fixed point the impurity spin is fully quenched: $T\chi_{\text{imp}} = 0$, $S_{\text{imp}} = 0$, and $C_{\text{imp}} = 0$. Remarkably, the leading corrections²⁶ here are $\Delta(T\chi_{\text{imp}}), \Delta S_{\text{imp}}, \Delta C_{\text{imp}} \propto T^{2r}$ for $0 < r \leq 1$, in other words, the impurity susceptibility $\chi_{\text{imp}}(T)$ vanishes as $T \rightarrow 0$ for $r > 1/2$.

We note that there exists a third stable fixed point of the pseudogap Kondo model, namely, a symmetric strong coupling fixed point. It is reached for pseudogap exponents $r < 1/2$ in the particle-hole symmetric case for sufficiently strong Kondo coupling; its thermodynamic properties are somewhat different from the ASC behavior quoted above.²⁶ However, the real materials are generically particle-hole asymmetric, and the physics of the particle-hole symmetric strong-coupling fixed point is of no relevance here.

B. Quantum-critical and crossover behavior

In this section, we focus on the properties of the impurity model in the vicinity of the quantum-critical point separating the local moment from the asymmetric strong-coupling phase. (Critical properties of the particle-hole symmetric pseudogap model are different, and were examined, e.g., in Refs. 22 and 24.)

In the vicinity of the critical point, one can define an energy scale T^* , which vanishes at the transition, and defines the crossover energy above which quantum-critical behavior is observed.⁶¹ If T^* is much smaller than both the bandwidth and the superconducting gap, we expect all observables to show a scaling behavior as a function of T/T^* and ω/T^* . Importantly, for the special case of $r = 1$, logarithmic corrections occur—strictly speaking, these corrections invalidate one-parameter scaling behavior since a second (high-energy) scale Λ (of order bandwidth) enters in the form of $\ln(T/\Lambda)$ or $\ln(\omega/\Lambda)$. However, for most practical purposes the logarithmic corrections are small, and in any case do not change the leading power-law behavior. We have ex-

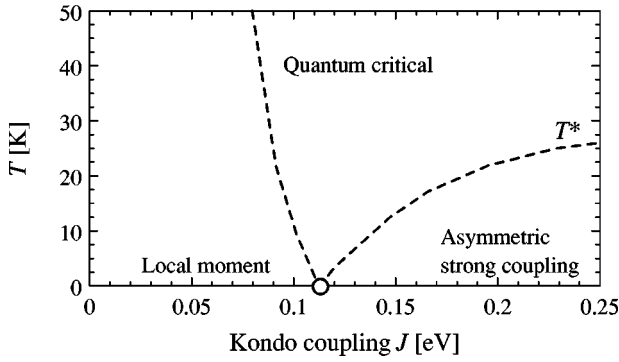


FIG. 2. Crossover diagram of the pseudogap Kondo model as function of the Kondo coupling J and temperature T , calculated with a pointlike impurity and a host band structure corresponding to a cuprate superconductor at optimal doping. The dot on the horizontal axis denotes the quantum phase transition between LM and ASC phases; the dashed lines are crossovers, indicating T^* . Both quantum-critical and local-moment regimes show a impurity susceptibility diverging as $1/T$, whereas in the asymmetric strong-coupling region the impurity susceptibility vanishes $\propto T$. As we will see in Sec. V, the critical Kondo coupling becomes significantly smaller for a spatially distributed impurity moment.

tracted the logarithmic corrections from the NRG results for some observables, and they are quoted below.

We start with the dependence of the cross over scale T^* on the reduced coupling, $j = (J - J_c)/J_c$, measuring the distance from the critical point at J_c . Our numerical results obtained by the NRG method are consistent with

$$T^* \propto j^{1/r} \quad (13)$$

for $1/2 < r \leq 1$ on both sides of the transition. In Fig. 2 we show numerical results for T^* for a high- T_c compound band structure at optimal doping. In Fig. 2 it is clearly seen that, even for Kondo couplings well away from J_c , the crossover scale T^* is small (20 K); therefore, impurity quantum-critical properties may easily be observed in the cuprates in a rather large temperature range without fine tuning. Parenthetically, we note that the crossover scale T^* is in general defined only up to a prefactor of order unity; in Fig. 2 the numerical value of T^* was taken from the location of the maximum in the T matrix spectral density (see below).

For $r=1$ the crossover temperature T^* vanishes linearly with the distance to the critical point (up to logarithmic corrections). This is in agreement with earlier NRG calculations²⁵ as well as the dynamic large- N approach.³⁰ However, it is at variance to the results obtained within the slave-boson mean-field approximation,²¹ which predicts an essential singularity for $r=1$, i.e., an exponentially vanishing scale T^* near the transition. We believe that the NRG prediction of a linearly vanishing T^* is correct (as the NRG method is reliable in capturing asymptotic low-energy physics), and that the exponentially vanishing scale is an artifact of the slave-boson method.

I. Susceptibility

As a first observable we consider the impurity susceptibility $\chi_{\text{imp}}(T)$. As a response function associated with a con-

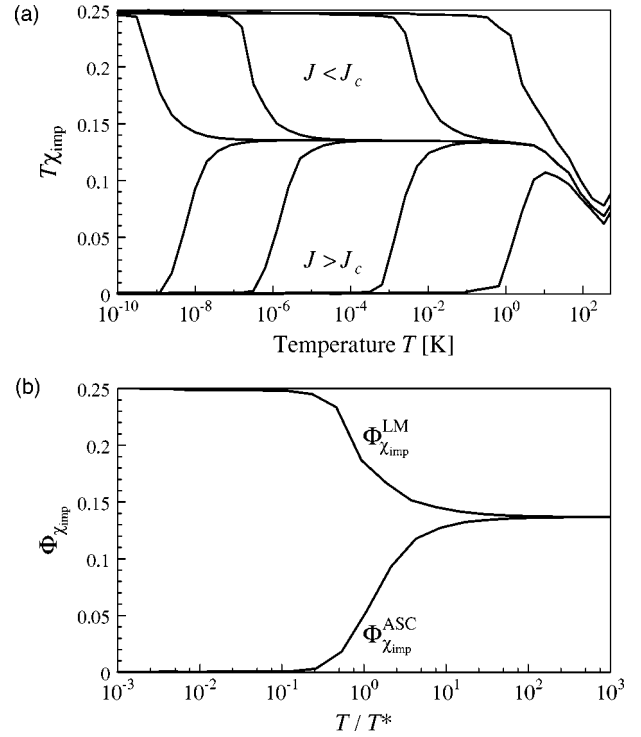


FIG. 3. (a) NRG results for the temperature dependence of $T\chi_{\text{imp}}$, for $r=1$, using a band structure corresponding to optimally doped cuprates. The different curves correspond to different values of the Kondo coupling J which are very close to the critical coupling $J_c \approx 0.11 \text{ eV}$. (b) Scaling function $\Phi_{\chi_{\text{imp}}}(T/T^*)$ extracted from NRG results, for $r=1$. (Possible logarithmic corrections violating scaling are very small here.) The value of T^* has been taken from the peak position in the impurity spectral density, see Sec. IV B 2.

served quantity, it cannot acquire an anomalous dimension;⁶² therefore, we expect precisely at the critical point a temperature dependence as

$$\chi_{\text{imp}}(T, J=J_c) = \frac{\mathcal{C}}{T}. \quad (14)$$

Here \mathcal{C} is a universal number, depending only on r . Interestingly, behavior (14) can be interpreted as the Curie response of an irrational spin. ($\mathcal{C}=1/4$ would correspond to the usual Curie response of a free spin $1/2$.) Numerical data for $T\chi_{\text{imp}}$ are shown in Fig. 3. In particular, close to J_c , there is a plateau in $T\chi_{\text{imp}}$, which allows one to extract the universal constant $\mathcal{C}(r=1) \approx 0.14$ in Eq. (14). This number is somewhat smaller than the value 0.164 quoted by Gonzalez-Buxton and Ingersent (see Fig. 14 of Ref. 26); this might be due to discretization or cutoff effects in the numerics (we have not attempted a careful finite-size analysis here).

The local susceptibility [Eq. (11)] is not protected by a conservation law, and can acquire an anomalous exponent η_{loc} . This implies a power law

$$\chi_{\text{loc}}(T, J=J_c) \propto T^{\eta_{\text{loc}}-1} \quad (15)$$

at the critical point.

For both finite T and finite $(J - J_c)$, the low-energy behavior is completely determined by the crossover energy scale T^* and the temperature T itself (up to logarithmic corrections for $r = 1$). Then the susceptibilities can be described by universal crossover functions

$$\chi_{\text{imp}}(T) = \frac{1}{T} \Phi_{\chi_{\text{imp}}} \left(\frac{T}{T^*} \right) = \frac{T^{2r-1}}{T^{*2r}} \bar{\Phi}_{\chi_{\text{imp}}} \left(\frac{T}{T^*} \right), \quad (16)$$

with $\bar{\Phi}_{\chi_{\text{imp}}}(x) = \Phi_{\chi_{\text{imp}}}(x)/x^{2r}$, and

$$\chi_{\text{loc}}(T) = \frac{\mathcal{B}}{T^{1-\eta_{\text{loc}}}} \Phi_{\chi_{\text{loc}}} \left(\frac{T}{T^*} \right) = \frac{\mathcal{B} T^{*\eta_{\text{loc}}}}{T} \bar{\Phi}_{\chi_{\text{loc}}} \left(\frac{T}{T^*} \right), \quad (17)$$

with $\bar{\Phi}_{\chi_{\text{loc}}}(x) = x^{\eta_{\text{loc}}} \Phi_{\chi_{\text{loc}}}(x)$, and \mathcal{B} an amplitude prefactor. Equations (16) and (17) define universal scaling functions Φ of the reduced temperature T/T^* ; the $\bar{\Phi}$ are, of course, different for different r 's and for both sides of the quantum phase transition, i.e., we have to distinguish Φ^{LM} and Φ^{ASC} . The scaling functions $\Phi_{\chi_{\text{imp}}}$ for $r = 1$ are shown in Fig. 3(b)—here our present numerics is not accurate enough to observe possible logarithmic corrections to scaling. Also, a reliable fitting of χ_{imp} to a Curie-Weiss law for a temperature range above T^* requires a finer discretization in the NRG procedure, and has not been attempted here. It is clear that the Weiss temperature will be approximately given by the crossover temperature T^* (defined by the T matrix peak), but we cannot give a reliable estimate for the ratio of the two.

We briefly discuss the asymptotics of the scaling functions Φ_{χ} . Spin quantization requires $\Phi_{\chi_{\text{imp}}}^{\text{LM}}(0) = 1/4$ and $\Phi_{\chi_{\text{imp}}}^{\text{ASC}}(0) = 0$; therefore, the zero-temperature limit of $T\chi_{\text{imp}}$ is fixed to $1/4$ throughout the whole local-moment phase (and to 0 in the whole ASC phase). The universal Curie response at the critical point [Eq. (14)] implies $\Phi_{\chi_{\text{imp}}}^{\text{ASC}}(\infty) = \Phi_{\chi_{\text{imp}}}^{\text{LM}}(\infty) = \mathcal{C}$. From $\chi_{\text{imp}}(T \rightarrow 0) \propto T^{2r-1}$ in the ASC phase we deduce $\Phi_{\chi_{\text{imp}}}^{\text{ASC}}(x) \propto x^{2r}$ for small x . This immediately gives $\chi_{\text{imp}}(T = 0) \propto T^{2r-1}/T^{*2r} \propto T^{2r-1}/(J - J_c)^2$ for $J > J_c$. However, the real superconductor will have a small residual DOS at the impurity site due to order-parameter relaxation; this will lead to a finite impurity susceptibility in the zero-temperature limit for $J > J_c$. Finally, NRG data²⁶ indicate that $\chi_{\text{loc}}(T \rightarrow 0) \propto 1/T$ in the LM regime; this gives us $\Phi_{\chi_{\text{loc}}}^{\text{LM}}(x) \propto x^{-\eta_{\text{loc}}}$, and therefore $T\chi_{\text{loc}}(T \rightarrow 0) \propto T^{*\eta_{\text{loc}}} \propto (J - J_c)^{\eta_{\text{loc}}/r}$ in the LM phase. Our preliminary NRG calculations of $T\chi_{\text{loc}}$ allowed us to extract the value of η_{loc} ; we found $\eta_{\text{loc}} \approx 0.05$ for $r = 1$.

At this point a few remarks about experimental susceptibility measurements and the possibility to observe the described quantum-critical behavior are in order. As detailed above, the only T dependence with a nontrivial power law can be expected in the local susceptibility $\chi_{\text{loc}}(T)$. However, a direct measurement of χ_{loc} requires a *local* field, and is perhaps only possible using muon spin resonance. In contrast, commonly used NMR techniques probe χ_{NMR} [Eq. (12)], and this quantity shows either a Curie law or saturates to a constant at low T . Measurements of the *total* suscepti-

bility in the local-moment regime should observe a Curie behavior, with the “full” prefactor corresponding to spin-1/2 per impurity, i.e., $\chi_{\text{imp}} = N_{\text{imp}}/4T$, where N_{imp} is the number of impurities. Such measurements have been performed on Zn-doped YBCO,¹⁰ and the results indicate a somewhat smaller value of the moment per impurity, which on the other hand depends only weakly on doping. Two explanations for the deviation from the $S = 1/2$ moment appear to be possible: Either there are subtle cancellation effects involved in the superconducting quantum interference device (SQUID) susceptibility measurements (one also has to keep in mind that the subtraction of the bulk susceptibility leads to rather large uncertainties in χ_{imp}), or the observed reduction of the moment reflects the quantum-critical behavior [Eq. (14)]. In the latter case, one should expect a crossover between the Curie law [Eq. (14)] to a Curie law with the “full” prefactor at low enough temperatures, i.e., for $T \ll T^*$, on the local-moment side of the Kondo phase transition. Experimentally, this would require measuring the total susceptibility well below the superconducting T_c on the underdoped side, and this has not been performed so far.

2. T matrix

We now turn to dynamic properties associated with the Kondo impurity; in particular we are interested in the conduction-electron T matrix. A knowledge of the T matrix is important for calculating the local density of states around the impurity, as observed in STM experiments. In the Anderson impurity model, the T matrix is connected to the impurity Green's function according to¹⁹

$$T(\omega) = V^2 G_{\text{imp}}(\omega). \quad (18)$$

We can define the T matrix spectral density as $\rho_T(\omega) = -\text{Im } T(\omega)/\pi$.

The behavior of the impurity spectral function was studied in the particle-hole symmetric pseudogap Anderson model in Ref. 24. In this case the strong-coupling behavior is different from the present asymmetric model, but the asymptotic local-moment behavior is identical—this is also seen in Fig. 1, where the particle-hole asymmetry flows to zero in the LM phase. For the LM regime it was found²⁴ that the impurity spectral density vanishes at the Fermi level as $|\omega|^r$; this could be verified in the present calculations. In the asymmetric strong-coupling regime we find a similar behavior, $\text{Im } G_{\text{imp}}(\omega) \propto \rho_T(\omega) \propto |\omega|^r$. Interestingly, the prefactor of this power law is equal for both positive and negative frequencies, meaning that the spectral asymmetry disappears in the scaling limit of $\text{Im } G_{\text{imp}}$ and ρ_T .

Of particular interest is the behavior of ρ_T in the quantum-critical region. From general scaling arguments, we expect a power law $\rho_T \propto \omega^{\eta_T-1}$, where η_T is the anomalous exponent. Our NRG results are consistent with such a power law, with $\eta_T = 1 - r$. So we have

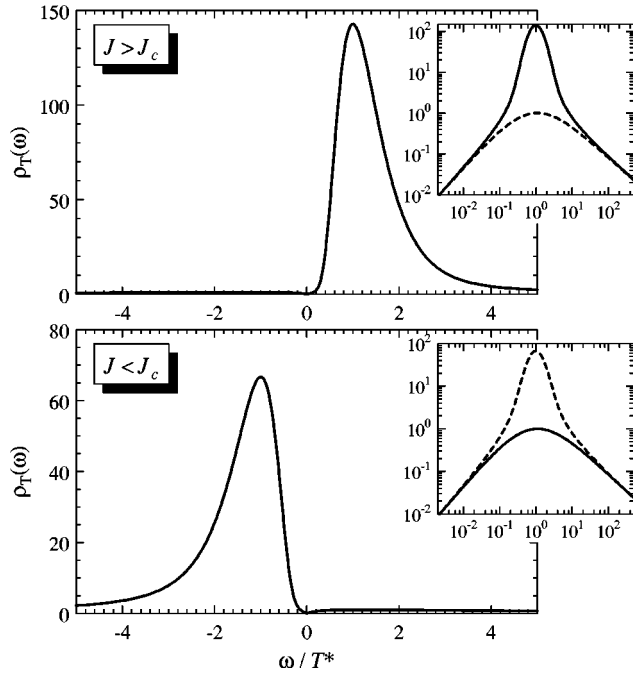


FIG. 4. Zero-temperature spectral densities ρ_T for the conduction electron T matrix at $r=1$, obtained by the NRG method. Upper panel: $J > J_c$, crossover from the ASC behavior at low energies to quantum criticality at high energies. Lower panel: $J < J_c$, i.e., crossover from the LM to quantum critical behavior. For comparison, the vertical axis has been normalized to the maximum value of ρ_T on the “nonpeak side.” Insets: same on a log-log scale, showing both $\bar{\omega} > 0$ (solid line) and $\bar{\omega} < 0$ (dashed line). Note that $\bar{\omega} > 0$ and $\bar{\omega} < 0$ are interchanged when the overall particle-hole asymmetry changes sign. If we ignore logarithmic corrections, the functions shown are equivalent to the imaginary part of the scaling function Φ_T .

$$\rho_T(\omega) \propto \frac{1}{\omega^r} \quad (r < 1),$$

$$\rho_T(\omega) \propto \frac{1}{\omega \ln^2(\Lambda/\omega)} \quad (r = 1). \quad (19)$$

Similar to the LM and ASC behaviors, any asymmetry drops out in the scaling limit of ρ_T , and the fixed-point spectral density is particle-hole symmetric.

As done for the susceptibilities, the crossover between the quantum-critical and the LM or ASC behavior in the T matrix can be described by a universal scaling function,

$$T(\omega) = \frac{\mathcal{A}}{T^{*r}} \Phi_T \left(\frac{\omega}{T^*}, \frac{T}{T^*} \right), \quad (20)$$

where \mathcal{A} is an amplitude prefactor, and Φ_T is a universal scaling function (for the particular value of r and for each side of the transition). For $r=1$ we have to keep in mind that logarithmic corrections spoil scaling, and a form like Eq. (20) is only approximately valid.

Numerical results for the $T=0$ impurity Green’s function for $r=1$ are shown in Fig. 4. They correspond to parameter

values very close to the transition, and represent the scaling functions Φ_T if we neglect logarithmic corrections. For $\bar{\omega} = \omega/T^* \ll 1$ we have an ASC behavior with $\text{Im}\Phi_T \sim |\bar{\omega}|$, for $\bar{\omega} \gg 1$, the spectral density follows the quantum-critical “power law” $|\bar{\omega}|^{-1} \ln^{-2}(\Lambda/\bar{\omega})$ as predicted above, with particle-hole symmetry in both limits. However, in the crossover region the asymmetry leads to a large peak for one sign of $\bar{\omega}$ (depending on the sign of the overall particle-hole asymmetry of the model)—this is true for both sides of the quantum phase transition.

In other words, the Kondo peak known from the metallic host Kondo model which is located at the Fermi level (in the scaling limit) is replaced by a peak at a *finite* energy—this energy actually corresponds to the crossover temperature T^* between the quantum-critical behavior and the LM or ASC behavior. For the crossover from critical to ASC behavior, one can identify T^* with the “Kondo” temperature of the problem, since a crossover from a Curie divergence to a constant (taking into account a small residual DOS) is seen in $\chi_{\text{imp}}(T)$ around T^* . In this paper, we have used the location of the peak in $\rho_T(\omega)$ (Fig. 4) as *definition* of T^* , as it is the numerically most convenient and precise criterion.

We note that very similar results for the T matrix were found in a recent dynamic large- N study of a multi-channel pseudogap Kondo model.³⁰ There it was possible to analytically determine the low-energy behavior of the quantities of interest, both at $T=0$ and finite T . Related observations were also made within slave-boson mean-field calculations.^{21,28}

We have also calculated the finite-temperature behavior of the impurity T matrix by the NRG method, for a fixed (temperature-independent) host density of states. It is worth emphasizing that the finite- T NRG method is a unique tool for this task, as the commonly used slave-boson method shows a spurious finite- T transition. A series of crossover functions for the spectral intensity is shown in Fig. 5. As expected, the peak is broadened, and loses spectral weight for $T \gg T^*$, whereas the peak position is nearly unaffected by changing T . The evolution of the weight under the peak (integrated from $\omega = -10T^*$ to $10T^*$) is shown in Fig. 6; similar to the usual Kondo effect the weight loss occurs rather slowly, e.g., the weight is reduced below 50% of its $T=0$ value only for $T > 5T^*$.

The results in Figs. 4 and 5 are possibly of relevance for the STM experiments done on Zn-doped BSCCO (Refs. 4 and 5)—the large peak in the differential conductance close to zero bias corresponds to the Kondo peak arising from the screening of the Zn-induced moment. We will discuss this issue further in Sec. V.

C. Location of the critical point

So far we have discussed magnetic screening in the pseudogap Kondo model for a fixed host density of states. Motivated by NMR experiments on Zn- and Li-doped cuprates, we now consider the dependence of the pseudogap Kondo effect on the hole doping level, i.e., with varying concentration of mobile carriers in the CuO_2 planes. Experimentally, a strong dependence of the Kondo temperature on

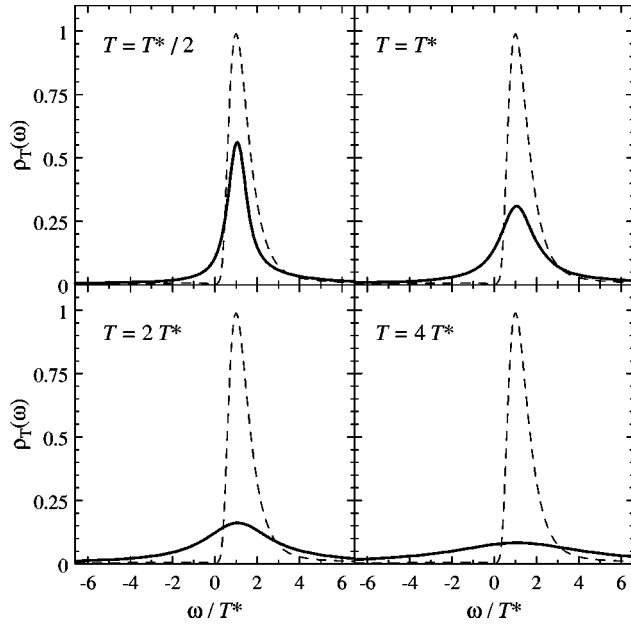


FIG. 5. Same as Fig. 4, but now for finite temperatures and $J > J_c$. The four panels show the evolution of the crossover peak for temperatures $T = T^*/2$, T^* , $2T^*$, and $4T^*$; the dashed line is the $T = 0$ result. The intensity has been normalized to the height of the $T = 0$ peak. The “Kondo” peak is broadened, and slowly loses weight for temperatures above T^* .

the doping level has been observed;^{12,13} in particular T_K appears to vanish in strongly underdoped samples.

As explained in Sec. I, a (boundary) transition between an unscreened moment for small doping and a screened (or even absent) moment for large doping can be anticipated on theoretical grounds. We propose that this transition corresponds to the quantum phase transition discussed above in the pseudogap Kondo model (also see Ref. 43), and we shall show numerical data indeed supporting that the transition in the pseudogap Kondo model can be driven by changing the doping level.

Doping in the cuprates (e.g., adding or removing oxygen in YCBO) is known to have a number of important effects, the main one of course being the change of the carrier concentration. For the pseudogap Kondo physics, the local den-

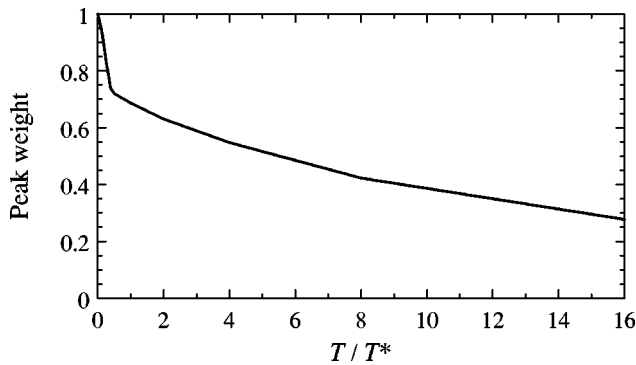


FIG. 6. Weight of the crossover peak as shown in Fig. 5, integrated from $\omega = -10T^*$ to $10T^*$, and normalized to the peak weight at $T = 0$.

sity of states is of particular importance. If we stick to the simple, doping-independent, tight-binding band structure used so far, then doping has two effects: (i) the change in the chemical potential, influencing carrier concentration and band asymmetry, (ii) the change in the magnitude of the d -wave gap as seen, e.g., in tunneling and photoemission experiments. As we will see, point (ii) is most important for the pseudogap Kondo physics, since a change in gap size immediately influences the low-energy part of the host DOS.

For BSCCO it was established from both ARPES (Ref. 59) and tunneling⁶⁰ measurements that the magnitude of the superconducting gap (as well as the normal-state pseudogap) changes considerably with doping: in contrast to T_c the gap increases in the underdoped regime, there taking up to twice of its value at optimal doping. For YBCO the situation is less clear, since high-quality tunneling or ARPES data are rare.⁶³ At least, thermodynamic measurements indicate an increase of the pseudogap temperature with decreasing doping in YBCO; therefore, a decrease of low-energy spectral weight similar to BSCCO is likely. In the following, we will use the doping-dependent gap values as measured in BSCCO,^{59,60} but we expect the results to reproduce the correct trend for most cuprates. The precise gap values used are $\Delta_0 = 55$, 38, and 23 meV for doping $\delta = 10\%$, 15%, and 20%. The host band structure entering Hamiltonian (1) is assumed to have a doping-independent tight-binding form, including longer-range hopping terms; we have performed calculations with the three parameter sets quoted in Table I of Ref. 51, as well as a simpler dispersion with $t = -0.15$ eV, $t' = -t/4$, and $t'' = t/12$, with qualitatively similar results. The employed densities of states are shown in Fig. 7(a) for underdoped and overdoped hosts; Fig. 7(b) shows the effective DOS “seen” by a four-site impurity (see Sec. V).

Of course one has to keep in mind that the evolution from the optimally doped d -wave superconductor to an insulator in the underdoped limit involves Mott physics which is not included in the simple one-particle description employed here. Therefore, the depletion of low-energy spectral weight, modeled here by an increasing d -wave gap, should be viewed as a phenomenological account for strong correlation effects.

NRG results for the doping dependence of the critical J_c are shown in Fig. 8, for both a single-site impurity and a spatially distributed four-site impurity (see Sec. V). The data show a 30–50% variation of the critical J , induced by the size change of the superconducting gap. For comparison we have also calculated the critical J with a doping-independent gap—the effect of the change in asymmetry is very small due to the presence of a finite asymmetry already at zero doping arising from hopping processes beyond nearest neighbors. In addition, we have checked that the change in the *form* of the superconducting gap as reported⁵⁹ for BSCCO, namely, the deviation from the $(\cos k_x - \cos k_y)$ form for underdoped samples, has only a weak effect on the critical J . We note that additional potential scattering terms of course modify the J_c values, but we have verified that, for moderate values of the bare scattering potential U , the trend that J_c increases for strong underdoping is preserved.

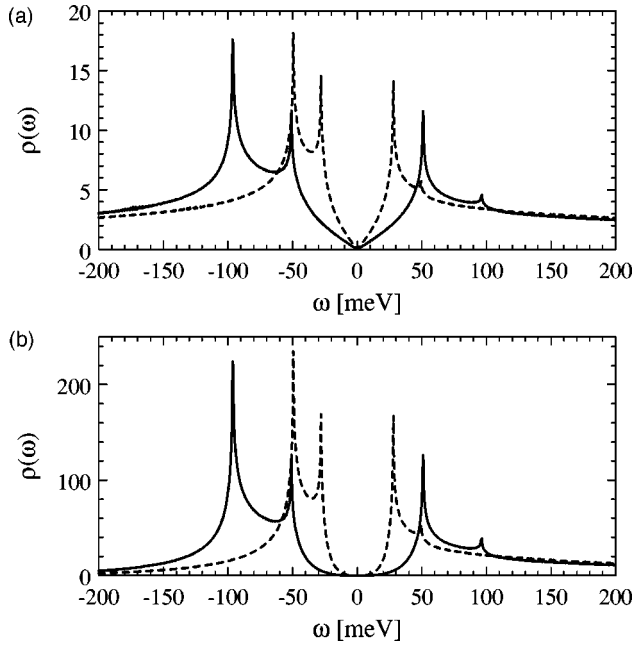


FIG. 7. Low-energy part of the input DOS used for the NRG calculations, here without potential scattering, $U=0$. Solid lines: 10% underdoped. Dashed lines: 19% overdoped. (a) DOS for a single-site impurity, being equivalent to the local DOS of the d -wave superconductor. (b) Effective DOS for a four-site impurity as discussed in Sec. V.

The main message of Fig. 8 is that J_c acquires a significant doping dependence, and has a value in the range of magnetic couplings which are expected in the cuprates. Of course, the precise form of the microscopic Hamiltonian describing the induced moment is not known, and therefore no estimate of the coupling value can be given. If we just assume a doping-independent Kondo coupling of a certain size, then we can obtain the values of the crossover temperature T^* from our NRG calculations. Sample data are shown in Fig. 9, and display a remarkable similarity to the NMR data of Refs. 12 and 13. The important result is that a *smooth* variation of the input parameters can lead to a *strongly* doping-dependent crossover (“Kondo”) temperature arising

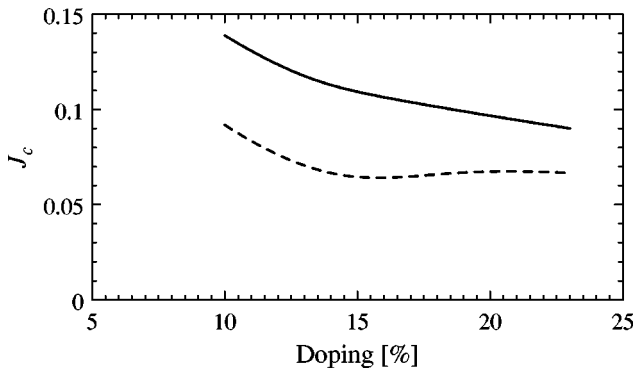


FIG. 8. Critical value of the Kondo coupling J_c vs doping, extracted from NRG calculations for a cuprate host DOS, with a doping-dependent superconducting gap. Solid line: single-site impurity. Dashed line: four-site impurity (see Sec. V).

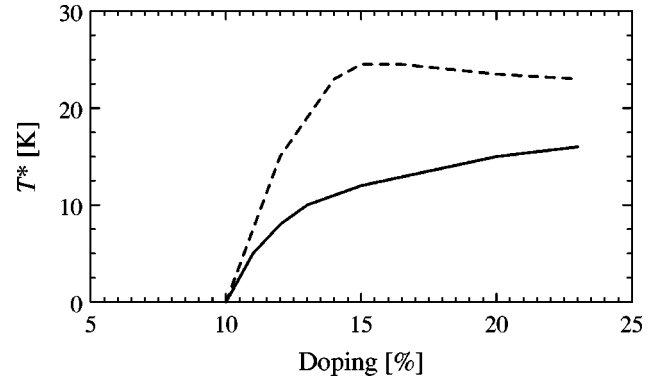


FIG. 9. Doping dependence of T^* describing the crossover from quantum-critical to asymmetric strong-coupling behavior, calculated with the band structures and gap values used for Fig. 8. For the impurity susceptibility the displayed T^* corresponds to the crossover from Curie-like behavior to a constant. Solid line: single-site impurity with $J=0.14$ eV. Dashed line: four-site impurity with $J=0.09$ eV.

from the vicinity to the boundary quantum phase transition. Therefore, the experimentally observed strong doping dependence of the NMR Weiss temperature^{12,13} is not necessarily an indication of a drastic change in the host electronic structure.

We close this section with a remark on the analytical understanding of the doping dependence of J_c as shown in Fig. 8. Certainly, the value of J_c will be mainly influenced by the low-energy part of the host density of states, but one can make this more precise, by trying to answer the question “which” electrons contribute to the Kondo screening in the pseudogap Kondo model. A rough estimate is provided by the expression for the critical coupling within the slave-boson mean-field approximation,

$$\frac{1}{J_c} \propto \int \frac{d\omega}{\omega} \rho_0(\omega), \quad (21)$$

with $\rho_0(\omega) \propto |\omega|^r$ being the host density of states. This integral is logarithmically divergent for $r=0$, indicating that the moment is always screened as $T \rightarrow 0$, and that this screening arises from host electrons close to the Fermi level. For $r > 0$, it is clear that *all* conduction electrons contribute to screening, with a weight proportional to $1/\omega$. Therefore, an estimate of J_c based on the low-energy part of ρ_0 only may not be appropriate. We note that a similar expression for J_c can be obtained within a dynamic large- N approach³⁰ to the pseudogap Kondo problem—there, ω in the denominator is replaced by $\omega^{1-\alpha}$, where α describes the anomalous exponent of the auxiliary fermion propagator at the critical point (with $\alpha \rightarrow 0$ for both $r \rightarrow 0$ and $r \rightarrow 1$, but nonzero in between).

D. Behavior above T_c

The numerical calculations in this paper are restricted to the d -wave superconducting state, but we want to give a brief comment on the normal-state impurity behavior. The NMR experiments in impurity-doped YBCO (Refs. 12 and 13) show enhanced Kondo screening above T_c —this is rather

natural as the superconducting gap disappears, the DOS near the Fermi level increases, and the metallic Kondo effect should be recovered.

Interestingly, no change in the magnetic properties is seen for underdoped samples when the temperature is tuned through T_c , i.e., the NMR susceptibility follows the same Curie law below and above T_c . Thus there is no Kondo screening even above T_c , which must be interpreted as a consequence of the celebrated pseudogap. The fact that no change at all occurs at T_c means that the depletion of low-energy spectral weight in both the superconducting and pseudogap phases is similar—this appears to support the speculation that the pseudogap and superconducting gap are of the same origin. Assuming that the normal-state pseudogap opens around optimal doping and follows the size of the superconducting gap for underdoped samples, we expect the *normal-state* Kondo temperature to follow a curve similar to Fig. 9, but with higher T_K values in the optimally doped regime. This was indeed found in Ref. 12.

V. EXTENDED MAGNETIC IMPURITIES WITH POTENTIAL SCATTERING

After having discussed general properties of the pseudogap Kondo model in the context of cuprate superconductors, we turn to a more detailed spatial modeling of nonmagnetic impurities inducing a magnetic moment. One important observation from NMR experiments^{11,14} is that these magnetic moments are not localized at the impurity site, but mainly on the nearest-neighbor copper sites. The simplest model for the induced moment is therefore a Kondo model of the form of Eq. (7),

$$\mathcal{H}_{\text{mag}} = \sum_{\mathbf{R}} J_{\mathbf{R}} \mathbf{S} \cdot \mathbf{s}_{\mathbf{R}}, \quad (22)$$

where the moment is coupled to the four Cu sites \mathbf{R} adjacent to the impurity, with $J_{\mathbf{R}} = J/4$.

An important point is that such a four-site Kondo model [Eq. (7)] is not a single-channel model, but instead has four screening channels associated with s -, p_x -, p_y -, and d -wave-like linear combinations of the conduction electrons on the four sites. These channels are not equivalent, and on general grounds one expects that the low-energy physics is dominated by the strongest screening channel. As our NRG cannot deal with a multichannel model, we have calculated the critical J values for the four channels separately, and found that the d -wave channel has the lowest critical J or, equivalently, the highest T^* for fixed J . The physics being dominated by this channel, it can be interpreted as the screening cloud having d -wave symmetry. Actually, the same conclusion was reached in a slave-boson treatment of the same model.⁴² We note that this d -wave symmetry is *not* directly related to the d -wave symmetry of the superconducting order parameter of the host—it is rather a band structure effect, and is completely determined by normal host Green's functions.

We have used such a four-site Kondo model in the d -wave channel to calculate the dashed curves shown in Figs. 8 and 9. The effective bath density of states seen by the impurity in this case is given by

$$\rho_{\text{eff}}(\omega) = -\frac{1}{\pi} \text{Im} \sum_{\mathbf{R}, \mathbf{R}'} \varphi_{\mathbf{R}} \varphi_{\mathbf{R}'} \text{Tr} \left[G(\mathbf{R}, \mathbf{R}', \omega) \frac{1 + \tau^z}{2} \right], \quad (23)$$

with $\varphi_{\mathbf{R}} = +[-]1$ for $\mathbf{R} - \mathbf{r}_0 = (\pm 1, 0)[(0, \pm 1)]$, and G is the Ψ Green's function [Eq. (3)] in Nambu notation. Examples are plotted in Fig. 7(b)—is it seen that the low-energy part close to the Fermi level is suppressed (actually, it follows an $|\omega|^3$ power law), whereas the weight at energies around the superconducting gap is strongly enhanced. This is easily understood if we consider the d -wave-like coupling of the impurity in momentum space: the “form factor” is $(2 + \cos 2k_x + \cos 2k_y - 4 \cos k_x \cos k_y)$; this expression vanishes along the diagonals of the Brillouin zone, but has maxima at $(\pi, 0)$ and $(0, \pi)$.

A second ingredient for an effective model describing nonmagnetic impurities is a potential scattering term [Eq. (2)]. This scattering potential is certainly well localized at the Zn or Li site; however, its bare value U is not known. Although certain experiments indicate that Zn behaves like a strong scatterer, this does not necessarily imply a large value of the bare scattering potential U , as the discussed Kondo screening can lead to strong scattering for low temperatures (note that T_K is much larger in the normal state, and can reach 150 K or more). Our results so far have been obtained with zero potential scattering U ; we have checked that the results are practically unchanged for U values up to $t/4$, and remain qualitatively valid for U up to $2t$. For larger values of the bare potential scattering, the critical J value for the pseudogap Kondo effect is significantly reduced, due to the increasing density of states near the Fermi level induced by the nearby scatterer.

Local density of states and STM

Recent STM experiments on Zn-doped BSCCO (Refs. 4 and 5) observed strong impurity-induced resonances in the differential conductance: for each impurity a huge peak close to zero bias (at roughly -1.5 meV) is found at a single location which has to be identified with the impurity site. This peak signal decays rapidly when moving away from the impurity, in addition it shows a checkerboardlike spatial modulation, i.e., it does not occur on the nearest neighbors of the impurity, but on the next-nearest neighbors and so on. This spatial shape is hard to explain with the assumption of strong potential scattering at the impurity site, because a large bare U would expel all electrons there and lead to a very small tunneling DOS exactly *at* the impurity site.

A possibility first discussed in Ref. 42 is that the huge peak close to zero bias arises from the Kondo screening of the Zn-induced moment; related studies can be found in Ref. 37. [In the STM context, it is important to distinguish between a screened moment which acts as a spin-independent resonant scatterer at low temperatures, and an unscreened moment (as in the case of Ni) which leads to spin-dependent scattering and causes a splitting of the impurity-induced peak in the local DOS.]

The local DOS probed by the STM tunneling experiment in the presence of both a potential scatterer and a Kondo impurity is obtained as

$$\rho_{\text{STM}}(\mathbf{R}, \omega) = -\frac{1}{\pi} \text{Im} \text{Tr} \left[\tilde{G}(\mathbf{R}, \mathbf{R}, \omega) \frac{1 + \tau^z}{2} \right], \quad (24)$$

where \tilde{G} is the full Ψ Green's function,

$$\begin{aligned} \tilde{G}(\mathbf{r}, \mathbf{r}', \omega) &= G(\mathbf{r}, \mathbf{r}', \omega) \\ &+ \sum_{\mathbf{s}, \mathbf{s}'} \varphi_{\mathbf{s}} \varphi_{\mathbf{s}'} G(\mathbf{r}, \mathbf{s}, \omega) \tau^z T(\omega) \tau^z G(\mathbf{s}', \mathbf{r}', \omega), \end{aligned} \quad (25)$$

with $T(\omega)$ being the Kondo impurity T matrix, and the \mathbf{s} sites are the neighbors of the impurity at \mathbf{r}_0 .

When comparing the results of microscopic calculations with STM data, one has to think about the actual tunneling path of electrons between the STM tip and the CuO_2 plane. BSCCO crystals are cleaved in such a way that a BiO layer forms the sample surface, and the electrons presumably tunnel via this BiO plane into the CuO_2 plane of interest. The nature of this tunneling path is not known. It was recently proposed^{64,65} that tunneling from the STM tip into a certain Bi orbital actually probes the electrons on the *neighboring* Cu $3d$ orbitals, leading to a strongly momentum-dependent tunneling matrix element. This so-called filter effect resolves the discrepancy between the observed spatial shape on the Zn resonance and the result expected from strong potential scattering. More precisely, the tunneling matrix elements proposed in Ref. 65 have a d -wave shape, such that the STM signal is given by the modified local density of states

$$\rho_{\text{STM}}(\mathbf{R}, \omega) = -\frac{1}{\pi} \text{Im} \sum_{\mathbf{R}', \mathbf{R}''} \bar{\varphi}_{\mathbf{R}'} \bar{\varphi}_{\mathbf{R}''} \text{Tr} \left[\tilde{G}(\mathbf{R}', \mathbf{R}'', \omega) \frac{1 + \tau^z}{2} \right], \quad (26)$$

replacing Eq. (24), with $\bar{\varphi}_{\mathbf{R}'} = +[-]1$ for $\mathbf{R}' - \mathbf{R} = (\pm 1, 0) \times [(0, \pm 1)]$. [Note the similarity to the effective DOS seen by the four-site impurity, Eq. (23).] At present, it is not clear whether such a filtering actually occurs, and further experiments are needed to clarify the tunneling path into the CuO_2 plane.

Reference 42 ignored this filter effect (as well as the possibility of strong potential scattering at the impurity site). We will show here that the results of Ref. 42 regarding the spatial shape of the impurity resonance are essentially unchanged for weak to moderate potential scattering, but change qualitatively for strong potential scattering. In the following, we will display the results of our calculations both with and without accounting for the possible filter effect.⁶⁵

Figure 10 shows the calculated tunneling spectra for a four-site Kondo impurity with zero (or weak) potential scattering. These data are similar to Fig. 1 of Ref. 42, but here the impurity properties are calculated using the NRG method, removing some artifacts of the slave-boson method, namely, overly large values of the critical coupling J_c , overly large Kondo temperatures for $J > J_c$, and overly sharp peaks in the T matrix. It is clearly seen that only the data in the left panel, i.e., without the filter effect, are consistent with the experimental observation,⁴ in that they show a large peak *at* the impurity site. Remarkably, the so-called coher-

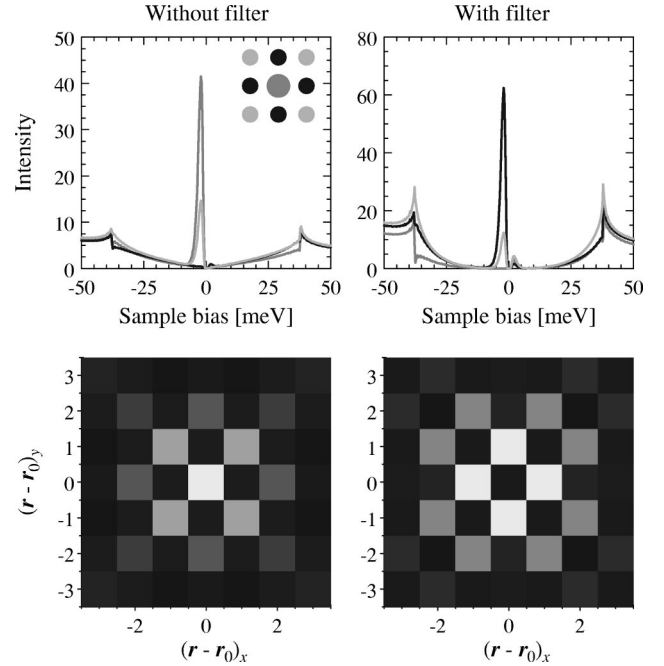


FIG. 10. Calculated tunneling density of states for the four-site Kondo impurity model at 15% hole doping with a realistic band structure ($t = -0.15$ eV, $t' = -t/4$, and $t'' = t/12$); $\Delta_0 = 0.04$ eV and $\mu = -0.14$ eV. The Kondo coupling is $J = 0.09$ eV, and the potential scattering $U = 0$. Top: local DOS vs energy for the impurity site and the nearest and second neighbor sites. Bottom: Spatial dependence of the local DOS at $\omega = -2$ meV. Left: local DOS in the CuO_2 plane. Right: local DOS after applying the filter effect proposed in Ref. 65.

ence peaks in the tunneling DOS at $\pm \Delta_0$ are almost completely suppressed near the impurity (cf. Fig. 7 for the bulk DOS) due to the interference between the bulk Green's functions and the impurity T matrix, although the superconducting order parameter is *not* changed (we did not account for gap relaxation). Therefore, the interpretation of suppressed coherence peaks in terms of locally suppressed superconductivity has to be used with care.

Switching on moderate potential scattering on the impurity site does not qualitatively modify the picture, as shown in Fig. 11. Note that for the chosen band structure and potential scattering value the global particle-hole asymmetry has changed its sign; therefore, the Kondo peak appears at the opposite side of the Fermi level compared to Fig. 10. (This should not be seen as a contradiction to the experiment, as the tight-binding band structure is a rough approximation to the real system, and the sign of the overall particle-hole asymmetry is not known.)

For huge values of potential scattering, the Kondo effect is heavily influenced in the present simple model. Due to the large scattering-induced DOS on the neighboring sites of the impurity the critical Kondo coupling is strongly reduced. Correspondingly the Kondo temperature for reasonable values of J (e.g., 50–100 meV) is increased to 100 K or more, which is in disagreement with the NMR observation.¹³ Therefore, we consider such a parameter combination unlikely to describe the experimental situation. Nevertheless,

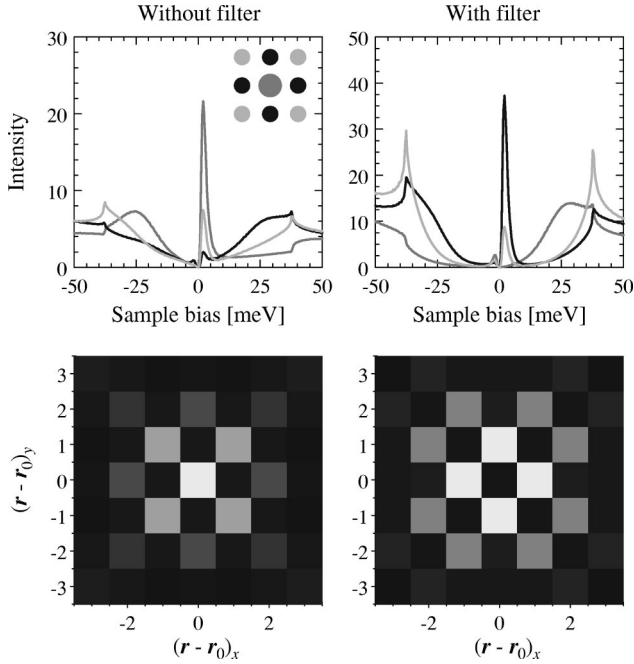


FIG. 11. Same as Fig. 10, but with potential scattering $U = |t| = 0.15$ eV. Here $J = 0.065$ eV. The lower panel shows the local DOS at $\omega = +2$ meV.

we have calculated the STM spectrum for such a case, shown in Fig. 12. We have chosen a smaller value of J , to obtain a Kondo temperature comparable to the experimental value. It is seen that a double-peak structure can occur. There are strong interference effects between the Kondo peak in the impurity T matrix and the potential scattering peak in the host DOS, with the result that the local (tunneling) DOS is

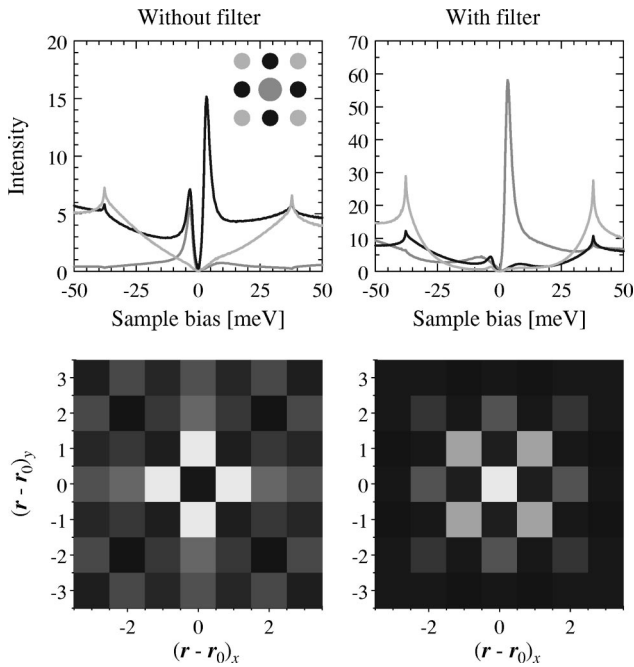


FIG. 12. Same as Fig. 10, but with potential scattering $U = 4|t| = 0.6$ eV. Here $J = 0.04$ eV. The lower panel shows the local DOS at $\omega = +3$ meV.

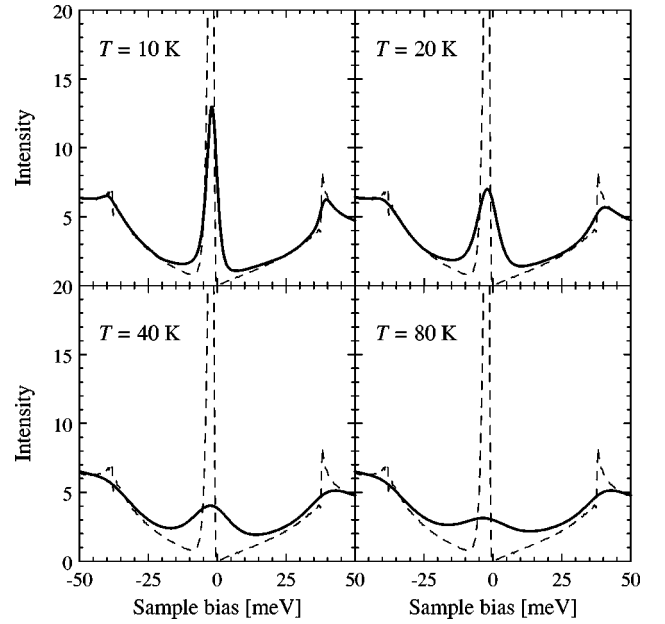


FIG. 13. Temperature evolution of the STM spectrum shown in Fig. 10, $T^* \approx 20$ K, calculated with a finite-temperature NRG method under the assumption of a T -independent host DOS. Shown is the tunneling DOS at the impurity site without applying the filter effect; the dashed line is the $T = 0$ result from Fig. 10. The thermal broadening of the signal due to the Fermi functions in both the tip and sample has been taken into account.

completely dominated by the potential scattering peak. The spatial shape of the resulting pattern is more compatible with the experiment after the filter effect is taken into account.

Last but not least, in Fig. 13 we show the temperature variation of the STM spectra for the situation in Fig. 10. In addition to the simple thermal broadening due to Fermi functions in the tip and sample, there is additional broadening and weight loss of the Kondo peak as shown in Fig. 5. Note that we have assumed a temperature-independent host DOS, which is approximately justified for temperatures up to $0.7T_c$. The broadening and loss of spectral weight occur rather gradually, and the peak will be seen also for temperatures well above T_K . If $T^* \approx T_K \approx 20$ K in optimally doped BSCCO, then the broadened Kondo peak will survive almost up to T_c . Near T_c the gap will close, T_K will increase,¹³ and the Kondo-induced peak might turn into a dip or Fano-like line shape as seen for Kondo impurities in metals.³² However, this signal will be broad and perhaps hard to observe.

Closing this section, we mention that there are subtleties in interpreting the NMR experiments^{11,14} in terms of a moment located on four sites (which lead to our simple effective model). The NMR experiments measure of course the fluctuating fields in the *full* system, whereas our model specifies the location of the *bare* moment. For a fair comparison one would have to calculate local NMR spectra after having accounted for the interaction of the moment with the host fermions (and possibly also with the antiferromagnetic spin fluctuations). This is possible in principle, but is left for future studies.

VI. CONCLUSIONS

In this paper, we have studied the dynamics of magnetic moments in high-temperature superconductors. We have focused on several aspects of the pseudogap Kondo model which describe the interaction of a localized spin with fermionic quasiparticles which obey a linearly vanishing density of states near the Fermi level. This Kondo problem shows a nontrivial boundary quantum phase transition as function of the Kondo coupling (or the size of the d -wave gap); we have examined a number of universal properties near this transition. We have argued that the quantum-critical behavior has consequences for susceptibility, NMR, and STM measurements in the cuprate superconductors. In particular, the crossover (“Kondo”) temperature T^* , as measured by NMR experiments, can acquire a strong doping dependence, due to the depletion of low-energy spectral weight with decreasing doping; and we have proposed that the observed vanishing of the Kondo temperature can be explained in terms of the quantum phase transition in the pseudogap Kondo model. The impurity T matrix which is observable via STM shows a large peak at a finite energy which coincides with the crossover temperature T^* .

Our calculated STM spectra are consistent with the experimental observation⁴ for small to moderate potential scattering values, and without taking into account the filter effect proposed in Ref. 65. Within our simple effective model, larger potential scattering values lead to Kondo temperatures at variance with the NMR results.¹³ Of course, we cannot exclude that the spatial distribution of the Zn-induced moment is different from what we have assumed, which would of course strongly affect the spatial shape of the STM resonance (but only weakly change the magnetic properties). One key experiment to decide whether the STM peak is of Kondo origin would be to measure its temperature evolution. Here the characteristic quantity is the spectral weight associated with the local Zn resonance. However, the weight loss with increasing T is rather slow (Figs. 5 and 6); therefore, high-quality measurements on impurities with small T_K (i.e., a small bias of the impurity resonance peak) are required.

The present NRG calculations for the pseudogap Kondo

model provide more reliable results than the common slave-boson mean-field approximation. This holds both for the qualitative behavior of the crossover scale T^* near the transition, and the quantitative results for the critical Kondo coupling and actual Kondo temperatures for parameters relevant for cuprates.

In the present work, we have neglected both the relaxation of the local superconducting order parameter around each impurity as well as interactions between the impurities. The latter are exponentially small in the impurity density, and are therefore unimportant for small impurity concentration (in the experimentally accessible temperature regime). The gap relaxation will mainly lead to a small residual low-energy DOS near the impurity, which causes Kondo screening at low enough temperatures even in the underdoped regime. However, the induced Kondo temperature is exponentially small in the residual DOS, and can be safely neglected.

Summarizing, our studies support that the NMR observations of Curie-Weiss-like behavior associated with Li or Zn impurities in high- T_c compounds can be described by the Kondo screening of the impurity-induced moments. The peak in the local DOS in Zn-doped BSCCO is likely of the same origin, but a number of experimental as well as theoretical issues remain to be resolved. We emphasize that the given numbers for Kondo couplings and characteristic temperatures can be viewed as rough estimates only, since the precise form of a Hamiltonian describing the impurity-induced moment is not known. Further theoretical studies should address the spatial dependence of NMR spectra (e.g., on the Y sites near the impurity), the additional coupling to antiferromagnetic fluctuations, as well as implications for transport measurements.

ACKNOWLEDGMENTS

We thank H. Alloul, A. V. Balatsky, J. Bobroff, S. Davis, M. Flatté, K. Ingersent, D. E. Logan, A. Matsuda, T. Pruschke, and N.-C. Yeh for helpful discussions, and especially S. Sachdev and A. Polkovnikov for collaboration on related work as well as numerous invaluable discussions. This research was supported by the DFG through SFB 484.

-
- ¹Y. Fukuzumi, K. Mizuhashi, K. Takenaka, and S. Uchida, Phys. Rev. Lett. **76**, 684 (1996); J. L. Tallon, C. Bernhard, G. V. M. Williams, and J. W. Loram, *ibid.* **79**, 5294 (1997); K. Karpinska, M. Z. Cieplak, S. Guha, A. Malinowski, T. Skoskiewicz, W. Plesiewicz, M. Berkowski, B. Boyce, T. R. Lemberger, and P. Lindenfeld, *ibid.* **84**, 155 (2000).
- ²F. Rullier-Albenque, P. A. Vieillefond, H. Alloul, A. W. Tyler, P. Lejay, and J.-F. Marucco, Europhys. Lett. **50**, 81 (2000); Y. Hanaki, Y. Ando, S. Ono, and J. Takeya, Phys. Rev. B **64**, 172514 (2001).
- ³H. F. Fong, P. Bourges, Y. Sidis, L. P. Regnault, J. Bossy, A. Ivanov, D. L. Millius, I. A. Aksay, and B. Keimer, Phys. Rev. Lett. **82**, 1939 (1999); Y. Sidis, P. Bourges, H. F. Fong, B. Keimer, L. P. Regnault, J. Bossy, A. Ivanov, B. Hennion, P. Gautier-

Picard, G. Collin, D. L. Millius, and I. A. Aksay, *ibid.* **84**, 5900 (2000).

⁴E. W. Hudson, S. H. Pan, A. K. Gupta, K. W. Ng, and J. C. Davis, Science **285**, 88 (1999); S. H. Pan, E. W. Hudson, K. M. Lang, H. Eisaki, S. Uchida, and J. C. Davis, Nature (London) **403**, 746 (2000).

⁵A. Yazdani, C. M. Howald, C. P. Lutz, A. Kapitulnik, and D. M. Eigler, Phys. Rev. Lett. **83**, 176 (1999).

⁶E. W. Hudson, K. M. Lang, V. Madhavan, S. H. Pan, H. Eisaki, S. Uchida, and J. C. Davis, Nature (London) **411**, 920 (2001).

⁷A. M. Finkelstein, V. E. Kataev, E. F. Kubovitskii, and G. B. Teitelbaum, Physica C **168**, 370 (1990).

⁸H. Alloul, P. Mendels, H. Casalta, J.-F. Marucco, and J. Arabski, Phys. Rev. Lett. **67**, 3140 (1991).

- ⁹A. V. Mahajan, H. Alloul, G. Collin, and J.-F. Marucco, Phys. Rev. Lett. **72**, 3100 (1994).
- ¹⁰P. Mendels, J. Bobroff, G. Collin, H. Alloul, M. Gabay, J.-F. Marucco, N. Blanchard, and B. Grenier, Europhys. Lett. **46**, 678 (1999).
- ¹¹A. V. Mahajan, H. Alloul, G. Collin, and J.-F. Marucco, Eur. Phys. J. B **13**, 457 (2000).
- ¹²J. Bobroff, W. A. MacFarlane, H. Alloul, P. Mendels, N. Blanchard, G. Collin, and J.-F. Marucco, Phys. Rev. Lett. **83**, 4381 (1999).
- ¹³J. Bobroff, H. Alloul, W. A. MacFarlane, P. Mendels, N. Blanchard, G. Collin, and J.-F. Marucco, Phys. Rev. Lett. **86**, 4116 (2001).
- ¹⁴M.-H. Julien, T. Feher, M. Horvatic, C. Berthier, O. N. Bakharev, P. Segransan, G. Collin, and J.-F. Marucco, Phys. Rev. Lett. **84**, 3422 (2000).
- ¹⁵This phenomenological view implies that it is possible to separate the formation of impurity moments from their interaction with the low-energy bulk excitations. As the moment formation is a high-energy phenomenon, this assumption appears justified regardless whether the moment is eventually screened or not.
- ¹⁶S. Sachdev, C. Buragohain, and M. Vojta, Science **286**, 2479 (1999); M. Vojta, C. Buragohain, and S. Sachdev, Phys. Rev. B **61**, 15152 (2000).
- ¹⁷J. L. Smith and Q. Si, cond-mat/9705140 (unpublished); Europhys. Lett. **45**, 228 (1999).
- ¹⁸A. M. Sengupta, Phys. Rev. B **61**, 4041 (2000).
- ¹⁹A. C. Hewson, *The Kondo Problem to Heavy Fermions* (Cambridge University Press, Cambridge, 1997).
- ²⁰D. Withoff and E. Fradkin, Phys. Rev. Lett. **64**, 1835 (1990); L. S. Borkowski and P. J. Hirschfeld, Phys. Rev. B **46**, 9274 (1992).
- ²¹C. R. Cassanello and E. Fradkin, Phys. Rev. B **53**, 15079 (1996); **56**, 11246 (1997).
- ²²K. Ingersent and Q. Si, cond-mat/9810226 (unpublished).
- ²³K. Chen and C. Jayaprakash, J. Phys.: Condens. Matter **7**, L491 (1995).
- ²⁴R. Bulla, T. Pruschke, and A. C. Hewson, J. Phys.: Condens. Matter **9**, 10463 (1997); R. Bulla, M. T. Glossop, D. E. Logan, and T. Pruschke, *ibid.* **12**, 4899 (2000).
- ²⁵K. Ingersent, Phys. Rev. B **54**, 11936 (1996).
- ²⁶C. Gonzalez-Buxton and K. Ingersent, Phys. Rev. B **57**, 14254 (1998).
- ²⁷D. E. Logan and M. T. Glossop, J. Phys.: Condens. Matter **12**, 985 (2000).
- ²⁸G.-M. Zhang, H. Hu, and L. Yu, Phys. Rev. Lett. **86**, 704 (2001).
- ²⁹A. Polkovnikov, cond-mat/0104485 (unpublished).
- ³⁰M. Vojta, Phys. Rev. Lett. **87**, 097202 (2001).
- ³¹N. Read and D. Newns, J. Phys. C **16**, 3273 (1983).
- ³²J. Li, W.-D. Schneider, R. Berndt, and B. Delley, Phys. Rev. Lett. **80**, 2893 (1998); V. Madhavan, W. Chen, T. Jamneala, M. F. Crommie, and N. S. Wingreen, Science **280**, 567 (1998).
- ³³O. Újsághy, J. Kroha, L. Szunyogh, and A. Zawadowski, Phys. Rev. Lett. **85**, 2557 (2000).
- ³⁴I. Martin and A. V. Balatsky, cond-mat/0003142 (unpublished).
- ³⁵A. V. Balatsky, M. I. Salkola, and A. Rosengren, Phys. Rev. B **51**, 15547 (1995); M. I. Salkola, A. V. Balatsky, and D. J. Scalapino, Phys. Rev. Lett. **77**, 1841 (1996).
- ³⁶H. Tsuchiura, Y. Tanaka, M. Ogata, and S. Kashiwaya, J. Phys. Soc. Jpn. **68**, 2510 (1999).
- ³⁷J.-X. Zhu and C. S. Ting, Phys. Rev. B **63**, 020506(R) (2001); **64**, 060501(R) (2001).
- ³⁸S. Haas and K. Maki, Phys. Rev. Lett. **85**, 2172 (2000).
- ³⁹W. A. Atkinson, P. J. Hirschfeld, A. H. MacDonald, and K. Ziegler, Phys. Rev. Lett. **85**, 3926 (2000).
- ⁴⁰If the host band structure is particle hole symmetric (not the case at optimal doping), the potential scattering (U in H_{imp}) has to be near infinity to obtain a low-energy quasibound state; however, in general, some finite and nonuniversal value of U is required.
- ⁴¹M. E. Flatté and J. M. Byers, Phys. Rev. Lett. **78**, 3761 (1997); M. E. Flatté, Phys. Rev. B **61**, 14920 (2000).
- ⁴²A. Polkovnikov, S. Sachdev, and M. Vojta, Phys. Rev. Lett. **86**, 296 (2001).
- ⁴³S. Sachdev and M. Vojta, *Proceedings of the XIII International Congress on Mathematical Physics, London, July 2000* [cond-mat/0009202 (unpublished)].
- ⁴⁴In numerical studies of finite-size t - J or Hubbard models with impurities, e.g., H. Tsuchiura, Y. Tanaka, M. Ogata, and S. Kashiwaya, Phys. Rev. Lett. **84**, 3165 (2000), one has to keep in mind that Kondo screening might not occur for small system sizes.
- ⁴⁵N. Read and S. Sachdev, Phys. Rev. Lett. **62**, 1694 (1989).
- ⁴⁶M. Milovanovic, S. Sachdev, and R. N. Bhatt, Phys. Rev. Lett. **63**, 82 (1989); S. Sachdev, Philos. Trans. R. Soc. London, Ser. A **356**, 173 (1998), and references therein.
- ⁴⁷N. Nagaosa and P. A. Lee, Phys. Rev. Lett. **79**, 3755 (1997).
- ⁴⁸C. Pépin and P. A. Lee, Phys. Rev. Lett. **81**, 2779 (1998).
- ⁴⁹G. Khaliullin, R. Kilian, S. Krivenko, and P. Fulde, Phys. Rev. B **56**, 11882 (1997); R. Kilian, S. Krivenko, G. Khaliullin, and P. Fulde, *ibid.* **59**, 14432 (1999).
- ⁵⁰S. Fujimoto, Phys. Rev. B **63**, 024406 (2001).
- ⁵¹M. R. Norman, Phys. Rev. B **63**, 092509 (2001).
- ⁵²P. Nozières and A. Blandin, J. Phys. (Paris) **41**, 193 (1980).
- ⁵³D. L. Cox and A. Zawadowski, Adv. Phys. **47**, 599 (1998).
- ⁵⁴P. Coleman and A. M. Tsvelik, Phys. Rev. B **57**, 12757 (1998).
- ⁵⁵K. Satori, H. Shiba, O. Sakai, and Y. Shimizu, J. Phys. Soc. Jpn. **61**, 3443 (1992).
- ⁵⁶K. G. Wilson, Rev. Mod. Phys. **47**, 773 (1975).
- ⁵⁷R. Bulla, T. A. Costi, and D. Vollhardt, Phys. Rev. B **64**, 045103 (2001).
- ⁵⁸The equivalence of the low-energy physics of Kondo and Anderson models requires a Kondo coupling J much less than the bandwidth, otherwise charge fluctuations in the corresponding Anderson model are not suppressed. It was noted in Ref. 26 that J values of order of the bandwidth are needed to reach the strong-coupling fixed point in the pseudogap Kondo model for $r > 1/2$, and that this physics can therefore not be realized in an Anderson model. However, Ref. 26 used a host DOS, where the power law extends to the band edges. In our situation, the range of the power-law dependence, i.e., the superconducting gap, is much smaller than the bandwidth, and the strong coupling phase can be reached with smaller J values. Our calculated J_c values provide an *a posteriori* justification, and we can conclude that for the parameters of interest the low-energy physics of Anderson and Kondo models are equivalent.
- ⁵⁹J. Mesot, M. R. Norman, H. Ding, M. Randeria, J. C. Campuzano, A. Paramakanti, H. M. Fretwell, A. Kaminski, T. Takeuchi, T. Yokoya, T. Sato, T. Takahashi, T. Mochiku, and K. Kadowaki, Phys. Rev. Lett. **83**, 840 (1999).

- ⁶⁰Ch. Renner, B. Revaz, J.-Y. Genoud, K. Kadowaki, and Ø. Fischer, Phys. Rev. Lett. **80**, 149 (1998); N. Miyakawa, J. F. Zasadzinski, L. Ozyuzer, P. Guptasarma, D. G. Hinks, C. Kendziora, and K. E. Gray, *ibid.* **83**, 1018 (1999); J. F. Zasadzinski, L. Ozyuzer, N. Miyakawa, K. E. Gray, D. G. Hinks, and C. Kendziora, *ibid.* **87**, 067005 (2001).
- ⁶¹S. Sachdev, *Quantum Phase Transitions* (Cambridge University Press, Cambridge, 1999).
- ⁶²See, e.g., S. Sachdev, Z. Phys. B: Condens. Matter **94**, 469 (1994).
- ⁶³Recent STM measurements indicated that the “size” of the superconducting gap in YBCO, defined as the distance between the so-called coherence peaks, is only weakly doping dependent. However, the *form* of the gap changes, indicating a depletion of low-energy weight with underdoping, being qualitatively consistent with what is assumed in Sec. IV C. See N.-C. Yeh, C.-T. Chen, G. Hammerl, J. Mannhart, A. Schmehl, C. W. Schneider, R. R. Schulz, S. Tajima, K. Yoshida, D. Garrigus, and M. Strasik, Phys. Rev. Lett. **87**, 087003 (2001).
- ⁶⁴J. X. Zhu, C. S. Ting, and C. R. Hu, Phys. Rev. B **62**, 6027 (2000).
- ⁶⁵I. Martin, A. V. Balatsky, and J. Zaanen, cond-mat/0012446 (unpublished).